

**SPECTROSCOPIC MEASUREMENTS OF
IMPURITY TEMPERATURES AND PARALLEL ION
FLOWS IN THE DIII-D DIVERTOR**

by
R.C. ISLER, N.H. BROOKS, W.P. WEST, A.W. LEONARD,
G.R. McKEE, and G.D. PORTER

JUNE 1998

DISCLAIMER

This report was prepared as an account of work sponsored by an agency of the United States Government. Neither the United States Government nor any agency thereof, nor any of their employees, makes any warranty, express or implied, or assumes any legal liability or responsibility for the accuracy, completeness, or usefulness of any information, apparatus, product, or process disclosed, or represents that its use would not infringe privately owned rights. Reference herein to any specific commercial product, process, or service by trade name, trademark, manufacturer, or otherwise, does not necessarily constitute or imply its endorsement, recommendation, or favoring by the United States Government or any agency thereof. The views and opinions of authors expressed herein do not necessarily state or reflect those of the United States Government or any agency thereof.

SPECTROSCOPIC MEASUREMENTS OF IMPURITY TEMPERATURES AND PARALLEL ION FLOWS IN THE DIII-D DIVERTOR

by

**R.C. ISLER,[†] N.H. BROOKS, W.P. WEST, A.W. LEONARD,
G.R. McKEE,[‡] and G.D. PORTER[◇]**

This is a preprint of a paper to be presented at the 13th International Conference on Plasma Surface Interactions on Controlled Fusion Devices, May 18–23, 1998, San Diego, California and to be published in *Journal of Nuclear Materials*.

[†]Oak Ridge National Laboratory

[‡]University of Wisconsin, Madison

[◇]Lawrence Livermore National Laboratory

**Work supported by
the U.S. Department of Energy
under Contracts DE-AC03-89ER51114, and DE-AC05-96OR22464**

**GA PROJECT 3466
JUNE 1998**

ABSTRACT

Impurity ion temperatures and parallel flow velocities in the DIII-D divertor have been measured from the shapes and shifts of visible spectral lines of C II, C III, and B II. Spectral multiplet patterns are analyzed by fitting them to theoretical profiles that incorporate exact calculations for the Zeeman/Paschen-Back effect. Ion temperatures range from 4–20 eV. Both normal flows toward the target plate and reversed flows away from the target plate are observed in the outer divertor leg; only flows toward the plate are detected in the inner leg.

1. INTRODUCTION

Divertor physics research has constituted one of the major efforts of the DIII-D tokamak program because of the importance of understanding how to manage particle and heat exhausts in power producing fusion devices. The extensive diagnostic array on this machine has made it possible to measure electron temperatures and densities [1] as well as radiative, conductive, and convective power losses [2,3]. Recently, efforts have been initiated both on DIII-D [4, 5] and elsewhere [6,7] to measure the flows of impurity and working gas ions which determine convective losses and which have a major influence on the efficiency of the divertor for shielding impurities from the core plasma. The visible spectrometer system, which has been used in the past to measure ion temperatures from Doppler broadening of spectral lines, has been upgraded so that ion flows along the field lines can be determined from Doppler shifts of the emission patterns. Impurity ion temperatures and parallel flow velocities have been measured under a wide variety of conditions; this paper presents some typical results, including the observation of theoretically predicted reverse flow regions.

2. EXPERIMENTAL APPARATUS AND VIEWING GEOMETRY

Spectra in the 4000 Å–9000 Å range are acquired by means of a 1.3 m Czerny-Turner multichordal divertor spectrometer (MDS) equipped with a 1200 l/mm grating. A two-dimensional CCD detector simultaneously records the input signals coming through twelve optical fibers at the entrance slit. The detector integration time is usually set at 125 ms. Figure 1 illustrates typical lines-of-sight for this system. The chords designated V1-V7 are nearly vertical and view the divertor floor through a port near the top of the vacuum vessel. The recently installed tangential views pass through a port near the bottom of the machine and are angled downward. Their projections on a poloidal plane are hyperbolic segments as shown by the curves labeled T2 and T4-T7, which represent five of the ten possible orientations available. Flow velocities along the tangential views are determined from Doppler shifts of emissions with respect to the lineshapes observed in the vertical views, which are essentially perpendicular to the magnetic field. These lines of sight, together with the ability to sweep the X-point radially, allow spectroscopic sampling of most of the divertor plasma. Two positions of the separatrix pertinent to the data discussed here are shown in Figs. 1(a) and 1(b).

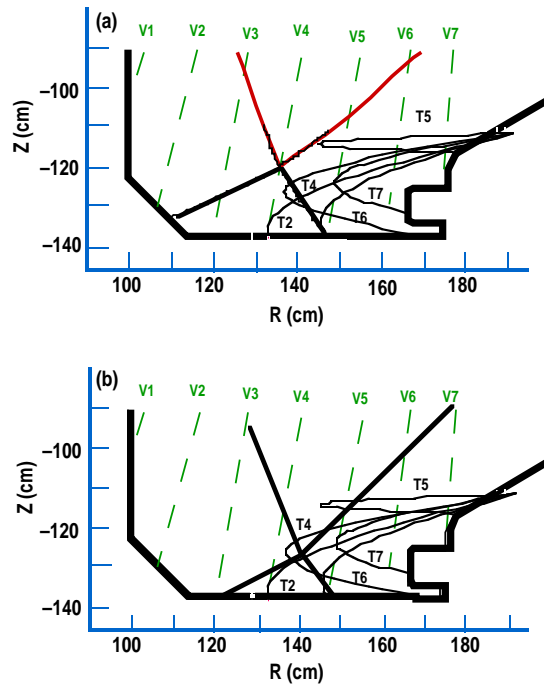


Fig. 1. Vertical views (V1–V7) and tangential views (T2, T4–T7) for obtaining the BII data employed in the present analysis. (a) separatrix configuration at 3.0 s. (b) separatrix configuration at 4.4 s.

3. ION TEMPERATURES

Very few impurity multiplets are usually intense enough to obtain accurate ion temperature and flow measurements. Most of the analyses of the ion characteristics have utilized the B II triplet ($^3P-^3S$) around 7335 Å, the C II doublet ($^2P-^2S$) near 6579 Å, and the C III triplet ($^3P-^3S$) near 4649 Å. Only temperatures determined from the vertical views are discussed in this section. These are believed to be more accurate than those deduced from the signals coming through the tangential views. This point will be discussed further in Section 4.

Because ion temperatures in the divertor are usually less than 20 eV, it is necessary to account accurately for the nonlinear splitting of the sublevels of excited electronic states in a magnetic field (Zeeman/Paschen-Back effect) when determining the Doppler widths [3,8]. Of all the transitions utilized for temperature measurements, deviations from a linear dependence on the field (Zeeman effect) appear most markedly in the B II multiplet, although they are evident in the other multiplets. Typical measurements from views V2 and V6 are shown by the solid circles in Fig. 2. In the absence of a magnetic field, this multiplet would appear as three closely spaced spectral lines, but the actual patterns are much more complicated and are qualitatively disparate in the two views because of the difference in field strength as a function of major radius. In order to obtain the maximum count rate, polarizers are not used in the optical path, therefore, the sum of the amplitudes of the sigma and pi components are equal. Ion temperatures are determined from the theoretical lineshapes that give the best fit to the entire multiplet for a given field strength. Since the spectroscopic signals are integrated over the entire sightline, it is not *a priori* evident that they will reflect a single temperature. However, both sets of data in Fig. 2 are well represented by profiles computed for a single ion temperature as shown by the solid curves. Low-field linear approximations of the theoretical profiles are shown as dashed curves to emphasize the necessity of including nonlinear effects into the analysis.

Time histories of two parameters characterizing the discharge (2.01 T, 1.36 MA) from which the data of Fig. 2 were recorded are shown in Fig. 3. Figure 3(a) illustrates the line averaged core density, and Fig. 3(b) displays the signal from a photomultiplier tube equipped with a filter to pass C III light. The field of view of the photomultiplier tube lies between views V4 and V5 of the MDS system. At 1.5 s a strong gas puff raises the density, and the neutral beam injection power is increased from 2.2 MW to 5 MW. The C III emission indicates the onset of a rapidly ELMIing H-mode at about the same time. The inner leg of the divertor is detached while the outer remains attached throughout the discharge.

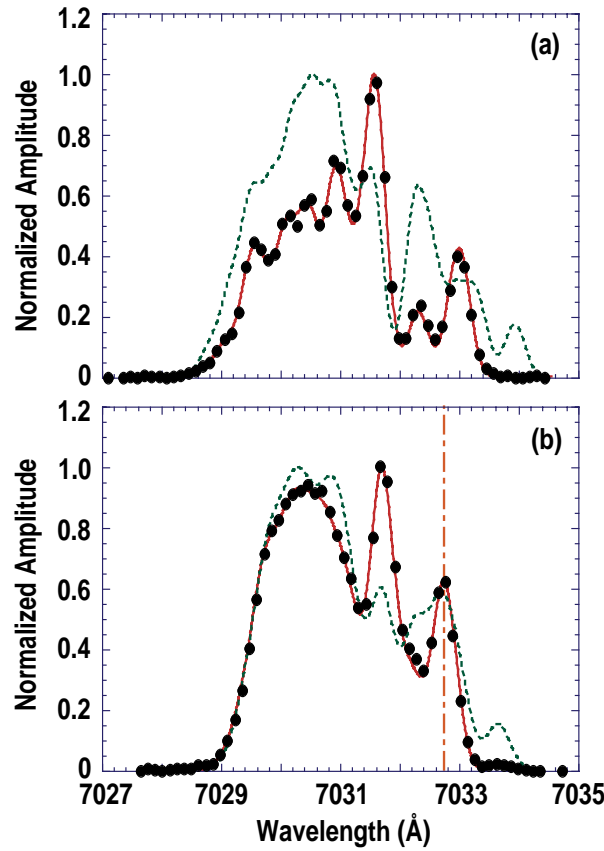


Fig. 2. Profiles of the B II ($3P-3S$) transition observed along views V2 (a) and V6 (b). Solid circles are measured data; solid lines are the best fit theoretical profiles using the Zeeman/Paschen-Back effect; dotted lines are theoretical profiles if only the low-field linear approximation (Zeeman effect) is employed.

B II temperatures as a function of time are shown in Fig. 4. From about 1.8–3.4 s no further major changes are made in operating conditions, and the temperatures vary little in each view. The highest temperatures, around 8 eV, are recorded from V5 which intercepts the outer strike point and from V7 which most likely detects its strongest signals upstream of the divertor region. Temperatures observed from the inner leg are in the 4–5 eV range. For strong signals, such as those shown in Fig. 2, the uncertainty in ion temperature appears to be 1 eV or less, which is evident in the small scatter of the data points during the quasisteady segment of the discharge. After 3.4 s the X-point is swept outward in major radius, and the temperature observed along some of the chords decreases. By 4.4 s V3 and V4 pass through the inner, rather than the outer leg [Fig. 1(b)], and the observed temperatures are the same as that along V2.

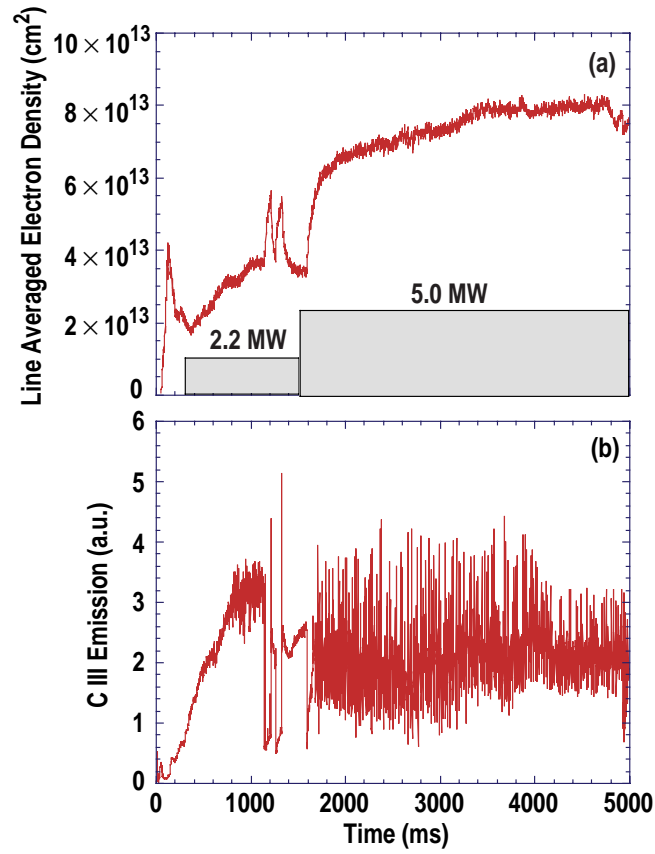


Fig. 3. (a) line-averaged core electron density and (b) divertor C III emission.

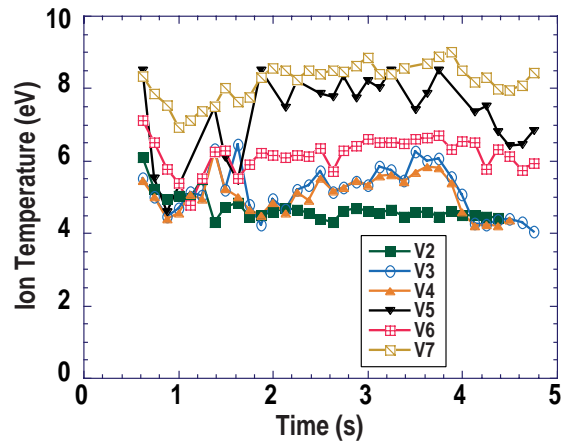


Fig. 4. Time histories of B II temperatures measured along the vertical views.

4. FLOW VELOCITIES

The flow velocities are determined from Doppler shifts of the emission patterns in the tangential views. Signals from view T2 at four different times for the discharge characterized in Fig. 3 are shown in Fig. 5. The sigma components strongly dominate these lineshapes so they do not resemble those from the vertical views. In general, the data points cannot be fitted by a single multiplet profile, but they can usually be fitted by two profiles with different Doppler shifts as shown by the dashed and dotted lines in Fig. 5. The solid lines are the sum of the two profiles. Although the theoretical fits are not perfect, they are close enough to the measured data to confirm that the major contributions to the signals come from two distinct groups of ions.

A qualitative indication of the shifts can be obtained from the fact that calculations show the peak at 7032.75 Å should appear at the same wavelength in views V6 and T2 if there is no parallel flow. The dot-dash vertical marker in Fig. 2(b) is located to pass through this local maximum. In Fig. 5(a) it is seen that this peak in the stronger component (dashed line) is blue-shifted with respect to the marker; in the DIII-D geometry a blue shift indicates that the group of ions providing the most intense emission is moving toward the target plate. However, the minor component is red-shifted and is indicative of a group of ions flowing in the reversed direction. This behavior, which is predicted theoretically to occur under certain circumstances [9], is generally observed in C II, C III, and B II during several types of discharge conditions. Specific modelling of C II behavior in attached DIII-D plasmas using the UEDGE code [10] do indeed indicate two intensity maxima near the locations inferred from experiment. The modeled velocity patterns are quite complex, but they show reversal near the separatrix while indicating normal flows can be present in the regions where they are observed by spectroscopy.

The presence of the reversed-flow component is even more obvious in Figs. 5(b) and 5(c) after the gas is added and the neutral beam injection power is increased. By 4.38 s the change of the magnetic configuration has positioned view T2 closer to the X-point [see Fig. 1(b)] where the intensity is stronger and the reversed component dominates the signal. Although the emitting ions may be distributed over several centimeters of the sightline, the variation of the multiplet patterns as a function of magnetic field strength makes it possible to determine the approximate radial locations of the most intense regions. For chords that cross the same radial location twice, the vertical position is ambiguous without supplementary data. The estimated error of the origin of signals shown in Fig. 5 is ± 5 cm, although the radiators often appear to be well enough localized that the position of the most intense group can be ascertained within ± 3 cm. The position of the weaker group may be less certain depending on signal strength.

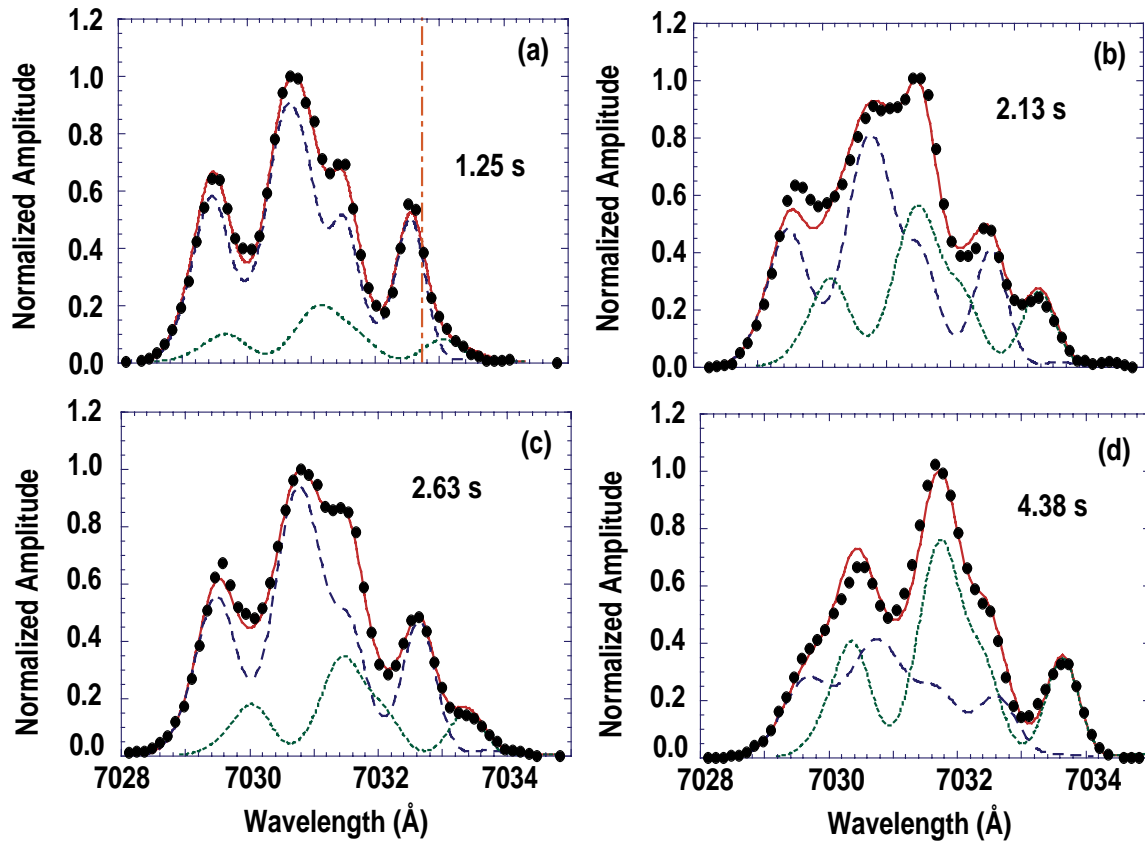


Fig. 5. Lineshapes of the B II doublet at 7035 Å observed along view T2 at four times. Solid points are measured data. The net theoretical curve (solid) is composed of blue-shifted (dashed) and red-shifted (dotted) components.

Table I shows velocities, Mach numbers, and most probable positions in major radius of the B II ions observed at the four times indicated in Fig. 5. The Mach numbers are computed with respect to the deuterium sound velocities by assuming an average temperature of 7 eV which corresponds to the B II ion temperatures in the outer leg as obtained from the vertical views. Ion temperatures interpreted from the tangential views are generally 2–4 eV greater than those from the vertical views. It is believed that this difference is an artifact caused by variations in the flow speed along the tangential lines-of-sight and by differences in the excited state sublevel splitting owing to the radial variation of the magnetic field. The possibility that the differences may be real cannot be completely ruled out, however. For most of the cases that have been analyzed, the normal-flow Mach numbers range from 0.3–0.7, whereas the reversed-flow values are near Mach 1. The radial locations shown in Table I are determined from the fact that the line shapes are sensitive to the magnetic field, but as already noted, they are not very precise for the B II data considered here. By referring to Fig. 1, it can be seen that the normal-flow group is interpreted to

be at major radii 15–20 cm to the low-field side of the separatrix. This conclusion is substantiated by the fact that intensities from the vertical views are by far the strongest along V6 which intercepts the target plate at a major radius of 162 cm (Fig. 1) in good agreement with the inferred radii of 1.58–1.64 m listed in Table I. The best fits to the data indicate that the reversed-flow group lies within a few cm of the separatrix.

Table I
Flow velocities, Mach numbers, and average positions for normal- and reversed-flow B II ions

Time (s)	Normal-Flow Ions			Reversed-Flow Ions		
	Velocity (10^6 cm/s)	Mach No.	Radius (m)	Velocity (10^6 cm/s)	Mach No.	Radius (m)
1.25	1.02	0.48	1.58	–0.51	0.24	1.34
2.13	0.75	0.35	1.58	–2.52	1.17	1.44
2.63	0.69	0.32	1.64	–2.09	0.98	1.49
4.38	1.27	0.59	1.64	–3.58	1.66	1.42

If the X–point is moved very far outward, the inner leg overlaps some of the tangential views. In many cases the radiation from a particular ion is much stronger in the inner leg than it is in the outer, and the normal-flow signals are red-shifted. In these cases inner leg flows can be distinguished, and the minor contribution to the red-shifted emission pattern from the reversed-flow ions on the outside does not significantly affect their velocity measurements. The magnitudes of these normal flow velocities tend to be comparable to those observed for the reversed group in the outer leg, *i.e.*, near Mach 1. If a group of reversed-flow ions exists on the inner leg it is probably impossible to extract its contribution from the total signal.

5. SUMMARY

Ion temperatures for B II, C II, and C III have been measured under a variety of conditions in the DIII-D divertor and are usually in the range of 4–20 eV. Velocities determined from Doppler shifts indicate that normal flows in the outer leg vary from $3 \times 10^5 - 1.5 \times 10^6$ cm/s (Mach 0.3–0.7) whereas on the inner leg they are $1 \times 10^6 - 3.5 \times 10^6$ cm/s (generally near Mach 1). Reversed flow regions exist in the outer leg during most types of operation, and the magnitude of their velocities tends to correspond to those of the normal flows on the inner leg. Although these results relate to data averaged over several ELMs [Fig. 3(b)], little difference has been detected for L-mode discharges in which ELMs are absent. For H-mode discharges with infrequent ELMs there is no difference between the normal flows in ELMing and quiescent periods, but the reversed-flow velocities are somewhat greater on average than during other types of operation.

REFERENCES

- [1] T.N. Carlstrom, C.L. Hsieh, R. Stockdale, D.G. Nilson, and D.N. Hill, *Rev. Sci. Instrum.* **68**, (1997) 1195.
- [2] A.W. Leonard, M.A. Mahdavi, S.L. Allen, N.H. Brooks, M.E. Fenstermacher, D.N. Hill, C.J. Lasnier, R. Maingi, G.D. Porter, T.W. Petrie, J.G. Watkins, and W.P. West, *Phys. Rev. Lett.* **78**, (1997) 4769.
- [3] R.C. Isler, R.D. Wood, C.C. Klepper, N.H. Brooks, M.E. Fenstermacher, and A.W. Leonard, *Physics of Plasmas* **4**, (1997) 355.
- [4] R.C. Isler, N.H. Brooks, W.P. West, A.W. Leonard, and G.R. McKee, "Normal and Reversed Impurity Flows in the DIII-D Divertor," General Atomics Report GA-A22815, March 1998.
- [5] J.A. Boedo, R. Lehmer, R.A. Moyer, J.G. Watkins, and D.N. Hill, *Bull. Am. Phys. Soc.* **42**, (1997) 1917.
- [6] J. Gafert, K. Behringer, D. Coster, C. Dom, K. Hirsch, M. Niethammer, U. Schumacher, and the ASDEX Upgrade team, *Plasma Phys. Control. Fusion* **39**, (1997) 1981.
- [7] B. LaBombard *et al.*, *J. Nucl. Phys.* **241-243**, (1997) 149.
- [8] J.D. Hey, Y.Y. Lie, D. Rusbüldt, and E. Hinz, *Contrib. to Plasma Phys.* **34**, (1994) 725.
- [9] P.C. Stangeby, J.D. Elder, D. Reiter, and G.P. Maddison, *Contrib. Plasma Phys.* **34**, (1994) 306.
- [10] T. Rognlien, J.L. Milovich, M.E. Resnik, and G.D. Porter, *J. Nucl. Mater* **196-198**, (1992) 347.

ACKNOWLEDGEMENTS

We would like to acknowledge several useful discussions with N. Wolf and M. Schaffer concerning theoretical and modelling aspects of particle flows in divertors. One of us (RCI) would also like to express his appreciation to E.A. Lazarus for providing a computer routine to calculate magnetic field strengths and direction cosines in DIII-D. This work was performed for the U.S. Department of Energy under contract numbers DE-AC05-96OR22464 with Oak Ridge National Laboratory, managed by Lockheed Martin Energy Research Corp. and DE-AC03-89ER51114 with General Atomics.